

# Non-equilibrium transport processes in a free-burning argon arc plasma under different operating pressures

Chuan Fang, Jian Chen, Heng Guo, Jing Li, He-Ping Li\*

*Department of Engineering Physics, Tsinghua University, Beijing 100084, P. R. China*

\* Corresponding author: liheping@tsinghua.edu.cn (H.-P. Li)

**Abstract:** Non-equilibrium is one of the intrinsic features of gas discharge plasmas. In this paper, the non-equilibrium transport processes in free-burning argon arc plasmas under different operating pressures are studied using a complete non-equilibrium physical-mathematical model. This is helpful for a deep understanding to the non-equilibrium synergistic transport mechanisms, as well as for tuning the key plasma parameters facing various applications, in collision-dominated plasmas.

**Keywords:** Non-equilibrium characteristics, synergistic transport mechanisms, arc plasma.

## 1. Introduction

Collision-dominated plasmas (CDPs) can be produced in a very wide range of operating parameters, including the operating pressure, the geometrical dimension of the plasma generator, the chemical composition of the plasma working gas, the driving frequency and amplitude of the discharge voltage / current of the power supply, etc. Consequently, the non-equilibrium mass-momentum-energy exchange (MMEE) processes will be quite different. This will definitely result in different non-equilibrium characteristics of the CDPs, e.g., different energy transfer channels between plasma and its environment and energy re-distributions among different energy states in plasmas [1]. Thus, the energy and species concentration levels in various CDPs will also be quite different. This would determine the applicability, treatment result and efficiency of a specific CDP source in a certain application filed.

In this paper, a free-burning arc plasma under different operating pressures is used as a model system to study the non-equilibrium synergistic MMEE processes in a CDP system. On one hand, as is known, arc plasmas are characterized by high gas temperatures / energy densities, heat fluxes, chemical activities, operation flexibilities, and are widely used in industries and aerospace, such as arc welding, plasma cutting, micro- or nano-scale materials processing, chemical production, waste treatment and thermal protection during the re-entry process of aerospace vehicles [2-7]. Thus, it is indispensable to improve the treatment quality and efficiency of arc plasmas in actual applications with the aid of monitoring and controlling of the key plasma parameters. On the other hand, most of the non-equilibrium features including the thermodynamic, chemical and electrical non-equilibria co-exist in the free-burning arc plasma. And it is very convenient to study these non-equilibrium features in a free-burning arc plasma due to the simple geometrical configuration of the plasma generator. That is to say, the free-burning arc can be considered as a model system for studying the non-equilibrium synergistic MMEE mechanisms in a CDP

system [8]. In this study, we focus on the non-equilibrium transport processes of the free-burning argon arcs under different operating pressures based on a complete set of non-equilibrium fluid model presented in Refs. [8-10].

## 2. Numerical Model

In this study, a free-burning argon arc is considered in which the species include electrons, argon atoms and singly ionized argon ions. The corresponding chemical reactions include the ionization and recombination processes, i.e.,  $\text{Ar} + e \leftrightarrow \text{Ar}^+ + 2e$ . The governing equations [8, 10] are listed as follows:

(1) Species mass conservation equation:

$$\bar{\nabla} \cdot (n_j \bar{v}_0) = -\bar{\nabla} \cdot (n_j \bar{V}_j) + \dot{n}_j \quad (1)$$

where  $n_j$ ,  $\bar{V}_j$  and  $\dot{n}_j$  are the number density, diffusion velocity and net production rate of species  $j$ . The subscript "j" indicates different particles in the system include electrons ( $e, j = 1$ ) and heavy particles ( $h, j > 1$ ), while  $\bar{v}_0$  is the mass-averaged velocity of the plasma system.

(2) Mass-averaged momentum conservation equation:

$$\bar{\nabla} \cdot (\rho \bar{v}_0 \bar{v}_0) = -\bar{\nabla} p + \bar{\nabla} \cdot \bar{\tau} + \bar{j} \times \bar{B} \quad (2)$$

where  $p$  and  $\bar{\tau}$  are the pressure and total viscous-stress tensor,  $\bar{j}$  is the total current density, and  $\bar{B}$  is the self-induced magnetic field.

(3) Energy conservation equation for electrons:

$$\bar{\nabla} \cdot \left[ \frac{5}{2} k_B n_e T_e (\bar{v}_0 + \bar{V}_e) \right] = \bar{\nabla} \cdot (\lambda_e \bar{\nabla} T_e) + \bar{\nabla} \cdot (\lambda_e^0 T_e \bar{\nabla} \ln \theta) - e n_e \bar{V}_e \cdot \bar{E} - Q_{ch}^{el} + Q_c^{inel} - U_R \quad (3)$$

(4) Energy conservation equation for heavy particles:

$$\bar{\nabla} \cdot \left\{ \frac{5}{2} k_B T_h \left[ n_a (\bar{v}_0 + \bar{V}_a) + n_i (\bar{v}_0 + \bar{V}_i) \right] \right\} = \bar{\nabla} \cdot (\lambda_h \bar{\nabla} T_h) + \bar{\nabla} \cdot \left[ (\lambda_i^0 + \lambda_a^0) T_c \bar{\nabla} \ln \theta \right] + e n_i \bar{V}_i \cdot \bar{E} + Q_{ch}^{el} + Q_h^{inel} \quad (4)$$

In Equations (3) and (4),  $k_B$  is the Boltzmann constant,  $\lambda_j$  and  $\lambda_j^0$  are the translational thermal conductivity and non-equilibrium thermal conductivity of electrons ( $j = e$ ) or

heavy species ( $j = h$ ),  $\theta$  is the temperature ratio, i.e.,  $\theta = T_e/T_h$ ,  $Q_{ch}^{el}$  is the rate of energy exchange per unit volume during elastic collisions between electrons and heavy particles,  $Q_j^{inel}$  is the rate of energy exchange per unit volume during inelastic collisions for electrons ( $j = e$ ) or heavy species ( $j = h$ ), while  $\vec{E}$  is the electric field.

(5) Poisson equation

$$\vec{\nabla} \cdot (\sigma \vec{\nabla} \phi) = 0 \quad (5)$$

where  $\sigma$  and  $\phi$  are the electric conductivity and potential of plasmas, respectively.

The database for the non-equilibrium transport properties of argon plasmas are obtained according to the calculation method presented in Ref. [9].

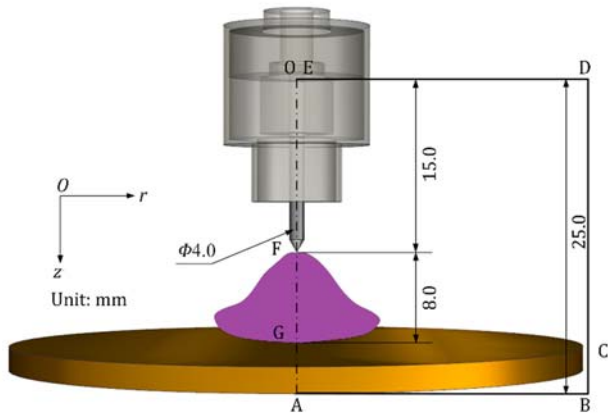


Fig. 1. Schematic of the calculation domain.

The calculation domain, A-B-C-D-E-O-F-G-A, is shown in Fig. 1. The distance between the two electrodes is 8.0 mm. In this study, the electrode surface temperature along OE and AB are set to be 500 K. The electric potential at the rear surface of the anode (AB) is set to be 0 V, while along the bottom of the cathode (OE), a uniform current density distribution is assumed. Along the plasma-electrode interfaces, a simplified sheath model is employed to satisfy the heat and current continuity conditions physically. The detailed descriptions on the boundary conditions and the sheath model can be found in Ref. [8].

### 3. Results and Discussions

With a constant arc current of  $I = 100$  A, the spatial distributions of the heavy-particle temperatures under the operating pressures of  $p = 0.1$  and 0.05 atm are shown in Fig. 2. It is seen from Fig. 2 and 3 that: (i) The highest temperature locates near the cathode tip due to the Joule heating effect with a higher current density for both cases. (ii) From the high temperature region to the cold gas region along the radial direction at a certain axial position (e.g.,  $z = 16.5$  mm), although both the heavy-particle temperature and electron temperature drop monotonously, the electron temperature decreases much more slowly than that of heavy particles in the radial range of 4.1~11.2 mm; and then, the electron temperature approaches to the heavy-

particle temperature quickly in the cold gas region ( $r > 11.2$  mm) due to the dominated recombination process of electrons with argon ions, as shown in Fig. 3. (iii) With the decrease of the operating pressure, the plasma expands radially leading to a larger non-equilibrium region, which is the so-called transition region as illustrated in Fig. 3. The widths of the transition region along the radial direction ( $\Delta r$ ) at  $z = 16.5$  mm under different operating pressures are shown in Fig. 4. It is seen clearly that with the increase of the operating pressure, the radial width of the transition region decreases. The possible reason is that the electrons collide with heavy particles more frequently and the energy exchanges between the two sub-systems of electrons and heavy particles also become much more intense at a higher pressure level.

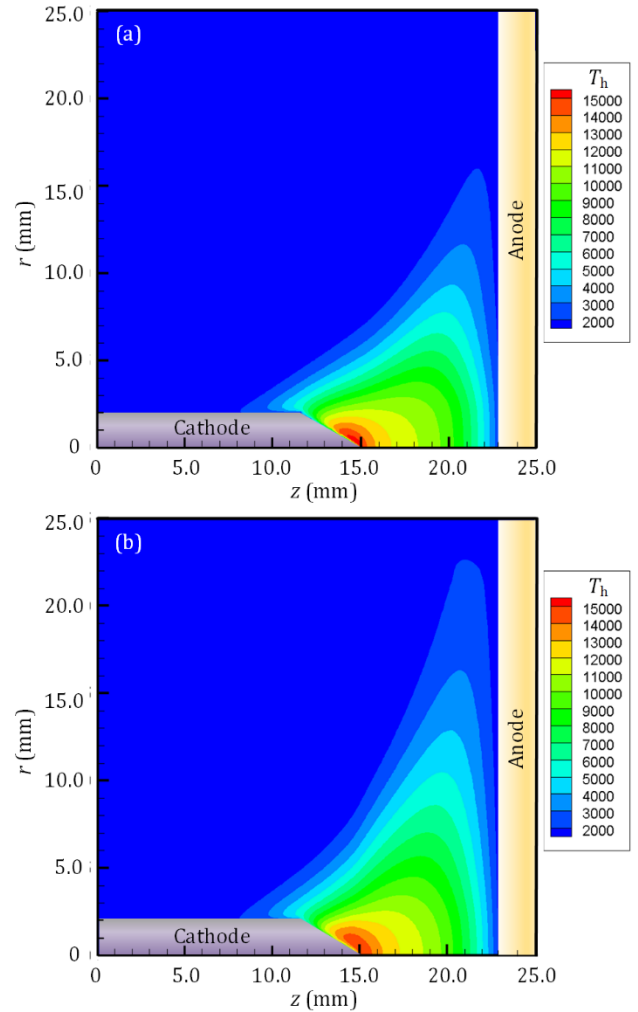


Fig. 2. Calculated spatial distributions of the heavy-particle temperatures at  $p = 0.1$  atm (a) and 0.05 atm (b).

### 4. Conclusions

In this paper, the non-equilibrium synergistic MMEE process in a free-burning argon arc plasma system is studied numerically based on a complete non-equilibrium fluid model. The preliminary modelling results show that the operating pressure has a significant influence on the non-equilibrium features of the arc plasmas with other

parameters being unchanged. It is indispensable to validate the modelling results by comparing with experimental measurement under the same operation conditions in future research.

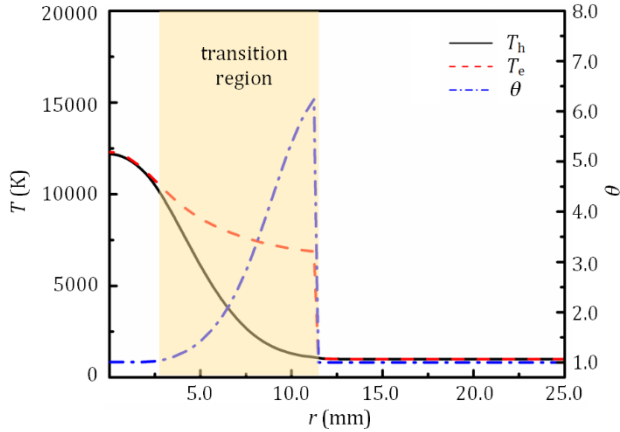


Fig. 3. Radial distributions  $T_h$ ,  $T_e$  and  $\theta$  at  $z = 16.5$  mm under  $p = 0.1$  atm.

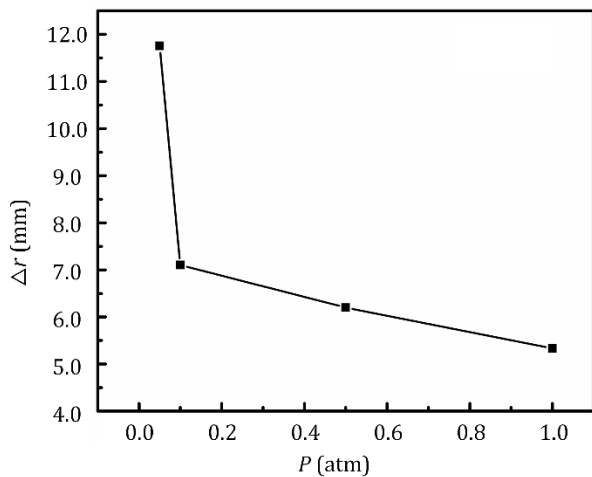


Fig. 4. Variation of the radial width of the transition region under different operating pressures.

### Acknowledgement

This work has been partly supported by the National Natural Science Foundation of China (Nos. 11775128, 11475103).

### References

- [1] H.-P. Li, K. Ostrikov, W. Sun, *Phys. Rep.*, **770-772**, 1 (2018).
- [2] A. B. Murphy, M. I. Boulos, V. Colombo, P. Fauchais, E. Ghedini, A. Gleizes, J. Mostaghimi, P. Proulx, D. C. Schram, *High Temp. Mater. Process.* **12**, 255 (2008).
- [3] P. Fauchais, T. Renault, N. Hussary, A. Refke, R. H. Henne, A. Hacala, C. D. Chapman, D. E. Deegan, M. Harabowsky, *High Temp. Mater. Process.* **12**, 165 (2008).
- [4] E. Pfender, *Plasma Chem. Plasma Process.* **19**, 1 (1999).
- [5] P. Fauchais, A. Vardelle, *Plasma Phys, Control. Fusion*, **42**, B365 (2000).

[6] P. Bletzinger, B. N. Ganguly, D. Van Wie, A. Garscadden, *J. Phys. D: Appl. Phys.* **38**, R33 (2005).

[7] I. V. Adamovich, I. Choi, N. Jiang, J.-H. Kim, S. Keshav, W. R. Lempert, E. Mintusov, M. Nishihara, M. Samimy, M. Uddi, *Plasma Sources Sci. Technol.* **18**, 034018 (2009).

[8] H. Guo, X.-N. Zhang, J. Chen, H.-P. Li, K. Ostrikov, *Sci. Rep.*, **8**, 4783 (2018).

[9] X.-N. Zhang, H.-P. Li, A. B. Murphy, W.-D. Xia, *Phys. Plasmas*, **20**, 033508 (2013).

[10] H.-P. Li, X.-N. Zhang, W.-D. Xia, *Phys. Plasmas*, **20**, 033509 (2013).